Mechanical Characterization of Differentiated Human Embryonic Stem Cells

Gidon Ofek

Vincent P. Willard

Department of Bioengineering,
Rice University,
Houston, TX 77005

Eugene J. Koay
Department of Bioengineering,
Rice University,
Houston, TX 77005;
Baylor College of Medicine,
Houston, TX 77030

Jerry C. Hu
Department of Bioengineering,
Rice University,
Houston, TX 77005

Patrick Lin
M.D. Anderson Cancer Center,
University of Texas,
Houston, TX 77050

Kyriacos A. Athanasiou[1]
Department of Bioengineering,
Rice University,
Houston, TX 77005
e-mail: athanasiou@rice.edu

Human embryonic stem cells (hESCs) possess an immense potential in a variety of regenerative applications. A firm understanding of hESC mechanics, on the single cell level, may provide great insight into the role of biophysical forces in the maintenance of cellular phenotype and elucidate mechanical cues promoting differentiation along various mesenchymal lineages. Moreover, cellular biomechanics can provide an additional tool for characterizing stem cells as they follow certain differentiation lineages, and thus may aid in identifying differentiated hESCs, which are most suitable for tissue engineering. This study examined the viscoelastic properties of single undifferentiated hESCs, chondrogenically differentiated hESC subpopulations, mesenchymal stem cells (MSCs), and articular chondrocytes (ACs). hESC chondrogenesis was induced using either transforming growth factor-β1 (TGF-β1) or knock out serum replacer as differentiation agents, and the resulting cell populations were separated based on density. All cell groups were mechanically tested using unconfined creep cytocompression. Analyses of subpopulations from all differentiation regimens resulted in a spectrum of mechanical and morphological properties spanning the range of hESCs to MSCs to ACs. Density separation was further successful in isolating cellular subpopulations with distinct mechanical properties. The instantaneous and relaxed moduli of subpopulations from TGF-β1 differentiation regimen were statistically greater than those of undifferentiated hESCs. In addition, two subpopulations from the TGF-β1 group were identified, which were not statistically different from native articular chondrocytes in their instantaneous and relaxed moduli, as well as their apparent viscosity. Identification of a differentiated hESC subpopulation with similar mechanical properties as native chondrocytes may provide an excellent cell source for tissue engineering applications. These cells will need to withstand any mechanical stimulation regimen employed to augment the mechanical and biochemical characteristics of the neotissue. Density separation was effective at purifying distinct populations of cells. A differentiated hESC subpopulation was identified with both similar mechanical and morphological characteristics as ACs. Future research may utilize this cell source in cartilage regeneration efforts. [DOI: 10.1115/1.3127262]

Keywords: cellular mechanics, biomechanics, chondrocyte, articular cartilage, unconfined cytocompression

1 Introduction

The biomechanical properties of single cells may significantly influence tissue development and homeostasis. The physical characteristics of individual cells play a vital role in the generation of local stress-strain fields within the cellular microenvironment [1] and the forces in turn experienced by the nucleus [2]. It has recently been observed that cellular mechanical properties may be indicative of phenotypic alterations within mesenchymal lineages [3,4]. Hence, cell biomechanical techniques have emerged as potential tools for the characterization and identification of cell populations during various developmental or differentiation processes. The most common of these biomechanic methodologies are atomic force microscopy [5], micropipette aspiration [6], cytoindentation [7], and unconfined cytocompression [8], which can yield the elastic or viscoelastic material properties of single cells given the assumptions of isotropy, incompressibility, and homogeneity.

Examining the mechanical properties of single human embryonic stem cells (hESCs) is of particular interest due to the pluripotent nature of these cells and their clear potential in an array of regenerative medicine applications. The prospect for using an abundant alternative cell source, such as hESCs, in tissue engineering is particularly appealing since this would obviate the common concerns of donor tissue scarcity or of dedifferentiation during autologous cell expansion [9]. Despite their potential, an examination of the mechanical properties of naive and differentiated hESCs has yet to be undertaken. An understanding of the mechanical characteristics of undifferentiated stem cells can greatly aid research investigating the forces necessary to promote differentiation into various cell lineages [10–14].

Embryonic stem cells have recently been utilized in cartilage tissue engineering efforts [15,16]. Studying the mechanical properties of chondro-induced hESCs may identify certain differentiated cell subpopulations that are most similar to native chondrocytes. It is believed that these cell subpopulations will be most suited for use in a tissue engineering approach for articular cartilage since they would be able to sustain similar in vivo mechanical loads. In addition, through an understanding of the mechanical properties of these differentiated cell groups, loading regimens can be determined, which elicit favorable biochemical [17,18] or behavioral responses [19], and thus promote neotissue growth.

[1]Corresponding author.

Contributed by the Bioengineering Division of ASME for publication in the JOURNAL OF BIOMECHANICAL ENGINEERING. Manuscript received November 5, 2008; final manuscript received March 9, 2009; published online May 8, 2009. Review conducted by Cheng Zhu.

 Copyright © 2009 by ASME

Downloaded From: http://biomechanical.asmedigitalcollection.asme.org/ on 06/19/2015 Terms of Use: http://asme.org/terms

Several differentiation strategies have been previously investigated to chondrogenically induce hESCs within embryoid body (EB) cultures [15,20–22]. Biochemical agents, such as transforming growth factor-β (TGF-β) [23], or media supplements, such as Invitrogen's knock out serum replacer (KOSR) (Invitrogen, Carlsbad, CA) [24], have been employed to promote the chondrogenic phenotype. However, a prevailing concern among the various approaches is the production of nonuniform cell populations postdifferentiation [25]. Thus, cell purification techniques are necessary to ensure that tissue engineered constructs are formed with homogeneous, chondrogenically differentiated hESCs. One such methodology, a Percoll gradient system, is capable of separating articular chondrocytes (ACs) based primarily on cell density, resulting in populations that differ in cell morphology, nucleus size, and protein synthesis [26,27]. Moreover, cell fractions originating from embryonic cells have shown significant differences in chondrogenic potential, both in monolayer and micromass cultures [28]. Therefore, it is of interest to examine potential differences in various chondro-induced hESC subpopulations, separated based on cell density.

The objectives of this study were to characterize the viscoelastic material properties of single hESCs and to identify mechanical differences between hESCs and their chondrogenically differentiated counterparts. Chondrogenesis was induced using two differentiation agents (TGF-β1 and KOSR), and the resulting cell populations were fractionated based on density. Mechanical properties of the undifferentiated hESCs and differentiated hESC cell subpopulations were measured using unconfined creep cytocompression [8]. We hypothesized that density separation of differentiated hESCs would yield subpopulations with different mechanical characteristics. We further hypothesized that a chondrogenically differentiated hESC subpopulation can be identified with stiffness properties and morphologies similar to those of native mesenchymal stem cells (MSCs) or ACs.

2 Materials and Methods

2.1 Chondrogenic Differentiation of Human Embryonic Stem Cells. The National Institute of Health (NIH) approved H9 hESC line (Wicell, Madison, WI) was cultured at passage 39 according to Wicell's instructions on irradiated CF-1 mouse embryonic fibroblasts (MEFs) (Charles River Laboratory, Wilmington, MA). Colonies were passaged using 0.1% type IV collagenase (Invitrogen, Carlsbad, CA) every 4–6 days. For the final passage prior to EB formation, colonies were passaged onto Matrigel (BD Biosciences, San Jose, CA) coated plates to reduce contamination of hESC colonies with feeder cells. While on Matrigel, the colonies were given MEF-conditioned medium. Once the hESC colonies on Matrigel reached 70–80% confluence, dispase (0.1% w/v in DMEM/F-12) was applied for 10–15 min to lift the hESC colonies from the culture dish. This left MEFs behind to form EBs from the hESC colonies [29]. After two washes with DMEM/F-12, the EBs were suspended in a chondrogenic medium containing either 1 ng/ml TGF-β1 (Peprotech, Rocky Hill, NJ) or 5% KOSR (Invitrogen, Carlsbad, CA). The base chondrogenic medium consisted of high-glucose Dulbecco's Modified Eagle Medium (DMEM) (Invitrogen, Carlsbad, CA), 10^{-7} M dexamethasone, insulin transferrin selenous acid + premix (6.25 ng/ml insulin, 6.25 mg transferrin, 6.25 ng/ml selenious acid, 1.25 mg/ml bovine serum albumin, and 5.35 mg/ml linoleic acid) (Collaborative Biomedical, San Jose, CA), 40 μg/ml L-proline, 50 μg/ml ascorbic acid, and 100 μg/ml sodium pyruvate. The EBs were then distributed into Petri dishes (Fisher, Hampton, NH) containing 15 ml of medium per dish. EBs were cultured for 3 weeks with media changes every 48 h.

2.2 EB Digestion and Density Separation. Density separation of differentiated hESCs was performed as described previously for chondrocytes [27] and heart mast cells [30]. Isotonic Percoll (Sigma, St. Louis, MO) was mixed with sterile phosphate buffered saline (PBS) (HyClone, Logan, UT) to produce a 60% stock solution. The stock was further diluted with PBS to produce Percoll solutions of 10%, 20%, 30%, 40%, 50%, and 60%. A preformed density gradient was created by sequentially layering 2 ml of each Percoll solution, starting with 60%, into a 15 ml conical bottom tube (VWR, Bridgeport, NJ). Two ml of DMEM containing the differentiated hESCs were carefully layered on top of the gradient, and the tube was centrifuged at $400\times$g for 20 min. After centrifugation, the cells collect at the interface between Percoll layers, which relate to their cellular density. The interface between each density layer was then isolated along with 1 ml of Percoll above and below each interface, using a sterile pipette. The Percoll was diluted with 8 ml of DMEM, centrifuged at $200\times$g, and the cell pellet was resuspended in 2 ml DMEM. Cells from each interface were counted with a hemocytometer.

2.3 MSC Culture and Articular Cartilage Isolation. Human MSCs from the bone marrow of one donor, age 35, were obtained from the Tulane Center for Gene Therapy (New Orleans, LA). Cells were seeded at 60 cells/cm^2 in T75 flasks (BD Biosciences, San Jose, CA) and cultured in α-MEM (modified eagle medium) (Invitrogen, Carlsbad, CA) containing 16.5% fetal bovine serum (FBS) (Atlanta Biologicals, Lawrenceville, GA), 4 mM L-glutamine, and 100 units/ml penicillin/streptomycin (Invitrogen, Carlsbad, CA). Cells were passaged every 7–10 days using 0.05% trypsin-EDTA (ethylenediaminetetraacetic acid)(Invitrogen, Carlsbad, CA) and replated into T75 flasks. The undifferentiated MSCs were used for the experiment at passage 4.

Human ACs were isolated from a healthy cartilage of one donor, age 25, excised as part of a surgery at M.D. Anderson Cancer Center (Houston, TX) to remove an osteosarcoma (Rice University IRB approval No. 08-115X). Articular cartilage tissue was digested overnight using 0.2% collagenase type II (w/v) (Worthington Biochemical Lakewood, NJ) in supplemented DMEM (0.1 mM non essential amino acids, 100U/ml penicillin/streptomycin, 0.25 μg/ml fungizone) at 37°C and 10% CO_2.

2.4 Cell Seeding. Isolated cells from each density layer were resuspended in their appropriate differentiation medium (TGF-β1 or KOSR) and seeded within a silicone isolator (PGC Scientifics, Gaithersburg, MD) onto a tissue culture dish to yield an approximate density of 3.8×10^4 cells/cm^2. Culture plates were incubated for 3–5 h at 37°C and 10% CO_2, to allow for proper cell attachment prior to cytocompression testing. Previous studies in our laboratory have shown that seeding time after a minimum of 3 h does not affect the viscoelastic properties of single cells [31,32]. The same seeding method was employed for undifferentiated hESC, human AC, and human MSC controls.

2.5 Creep Cytocompression. Unconfined creep cytocompression experiments were performed on each experimental group ($n>10$ cells/group) using the same medium as the seeding phase, supplemented with 4-(2-hydroxyethyl)-1-piperazineethanesulfonic acid (HEPES) buffer (Fisher Scientific, Pittsburgh, PA) to prevent *p*H changes while the culture dish was exposed to ambient conditions. A previously validated creep cytoindentation apparatus [7,8] was used to apply controlled stresses onto single adherent cells via a 50.8 μm diameter tungsten probe. Cells were positioned directly below the probe, as confirmed through visualization on an inverted microscope. The compressing tip was driven toward the cell by vertical control over the far end of the probe using a piezoelectric actuator. A laser displacement meter simultaneously tracked the true position of the probe tip (Fig. 1). Before each trial, the system was calibrated by comparing known piezoelectric displacements with recorded measurements from the laser micrometer. During cytocompression, the deflection of the probe (δ) was calculated based on the differences in piezoelectric movement and laser displacement measurements. Cantilever beam theory was then used to calculate the reaction force by the cell, based on known physical parameters of the

Downloaded From: http://biomechanical.asmedigitalcollection.asme.org/ on 06/19/2015 Terms of Use: http://asme.org/terms

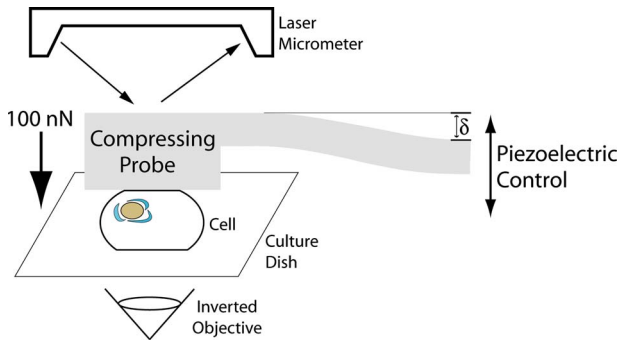

Fig. 1 Illustration of the creep cytocompression apparatus. A piezoelectric actuator drives a 50.8 μm tungsten probe axially toward cells seeded onto a culture dish and the free end of the probe is simultaneously tracked by a laser micrometer. The difference in recorded displacement by the laser micrometer and piezoelectric motor results in a probe deflection (δ), which is correlated with a reaction force using cantilever beam theory. Through a negative feedback algorithm, the position of the probe is continuously altered to hold a step load of 100 nN onto the single cells. An inverted objective located below the stage is used to position the probe and the cell, as well as measure cell diameters.

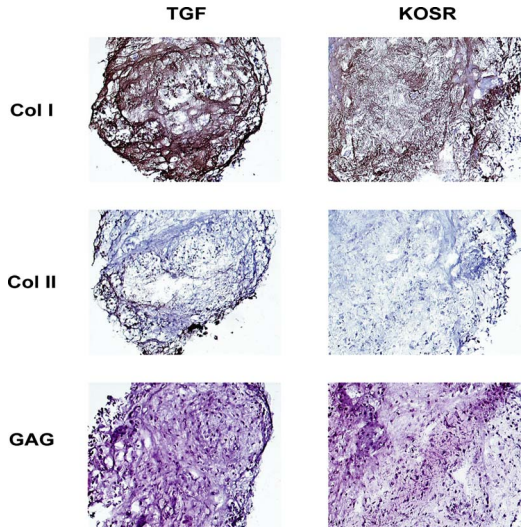

Fig. 2 Histological sections of EBs differentiated with TGF-β1 (column 1) and KOSR (column 2). Original magnification, 40X. Collagen type I, collagen type II, and s-GAGs were all present, indicating a cartilaginous differentiation of the hESCs.

tungsten probe and the measured deflection distances. Finally, a closed-loop algorithm was employed to maintain a constant force level of 100 nN onto each cell for 30 s by appropriately moving the piezoelectric actuator. Cell diameter was measured with a reticle in the microscope objective. Applied stress was defined as the force divided by the maximum cell diameter. Cell height was determined by measuring the contact distance between the probe and the culture dish after each test, and comparing it to the contact distance of the cell.

2.6 Viscoelastic Properties. The unconfined compression creep behavior of single cells was fitted to a standard linear viscoelastic solid model. Previous work has shown that the viscoelastic model accurately depicts the initial creep behavior of single chondrocytes [8]. Briefly, this model considers the cell to be an isotropic, homogeneous, and incompressible viscoelastic solid undergoing small deformations. It yields three unique material properties: instantaneous modulus (E_o), relaxed modulus (E_∞), and apparent viscosity (μ). The experimental deformation behavior of single cells over time was analyzed using the following equations:

$$u(t) = \frac{2\sigma h_o}{3E_\infty}\left[1 + \left(\frac{\tau_\varepsilon}{\tau_\sigma} - 1\right)e^{-t/\tau_\sigma}\right]H(t) \quad (1)$$

$$E_o = \frac{\tau_\sigma}{\tau_\varepsilon}E_\infty \quad (2)$$

$$\mu = \tau_\varepsilon(E_o - E_\infty) \quad (3)$$

where $u(t)$ is the cell deformation over time, σ is the applied constant stress, h_o is the initial cell height, $H(t)$ is the step function, and τ_ε and τ_σ are the stress and creep relaxation time constants, respectively. Creep curves were fitted to this viscoelastic model using MATLAB 6.5 (The MathWorks, Natick, MA), via the nonlinear Levenburg–Marquardt method.

2.7 Histology and Immunohistochemistry. To confirm cartilaginous differentiation of the hESCs, representative EBs from the TGF-β1 and KOSR groups were frozen in cryoembedding medium and sectioned at 12 μm thicknesses. Safranin-O and fast green staining was used to examine the presence of sulfated glycosaminoglycans (s-GAGs) [33]. Additional slides were processed with immunohistochemistry (IHC) analyses to visualize collagen types I and II. Briefly, these slides were fixed in chilled acetone, quenched of exogenous peroxidase activity with 3% H_2O_2 in methanol, blocked with serum (Vectastain ABC kit, Burlingame, CA), and incubated with either mouse anticollagen type I antibody (Axell, Westbury, N.Y.) or rabbit anticollagen type II antibody (Cederlane, Burlington, NC). The appropriate mouse or rabbit secondary antibody (Vectastain ABC kit) was applied, followed by the avidin-biotinylated enzyme complex (Vectastain ABC kit), diaminobenzidine (DAB) reagent (Vector Labs, Burlingame, CA), and hematoxylin counterstain to visualize nuclei. Native tendon and articular cartilage served as positive and negative controls. To assess if the hESCs had differentiated along other mesenchymal lineages, additional slides were processed with Von Kossa and oil red O stains for mineralization and adipose tissue, respectively.

2.8 Data Analysis. Analysis of variance was used to discern differences in mechanical properties among all differentiated hESC and control groups, with a Tukey's post hoc test when warranted. Significance was defined as $p < 0.05$ throughout the study.

3 Results

3.1 hESC Differentiation and Density Separation. Positive staining was observed for s-GAGs, and collagen types I and II in EBs from both TGF-β1 and KOSR differentiation regimens (Fig. 2), suggesting a cartilaginous differentiation. Staining with Von Kossa and oil red O was negative (data not shown), indicating the absence of undesired differentiation. Subpopulations of chondrogenically differentiated hESCs were isolated based on cell density (Fig. 3). In the TGF-β1 group, cells were identified within 10–20% (TGF 10-20), 20–30% (TGF 20-30), 30–40% (TGF 30-40), 40–50% (TGF 40-50), and 50–60% (TGF 50-60) density interfaces, respectively. In the KOSR group, cells also fell within 10–20% (KOSR 10-20), 20–30% (KOSR 20-30), 30–40% (KOSR 30-40), 40–50% (KOSR 40-50), and 50–60% (KOSR 50-60) density interfaces, respectively. The percentage of cells isolated at each Percoll density interface for both differentiation regimens is given in Table 1. Due to the low cell yield in the TGF 10-20, KOSR 10-20, KOSR 40-50, TGF 50-60, and KOSR 50-60 groups, mechanical testing of these subpopulations was not possible.

3.2 Viscoelastic Properties and Cell Morphologies. The deformation behavior of single cells in response to a 100 nN step load was fitted to a viscoelastic model (Eqs. (1)–(3)) to yield an instantaneous modulus, relaxed modulus, and apparent viscosity.

Downloaded From: http://biomechanical.asmedigitalcollection.asme.org/ on 06/19/2015 Terms of Use: http://asme.org/terms

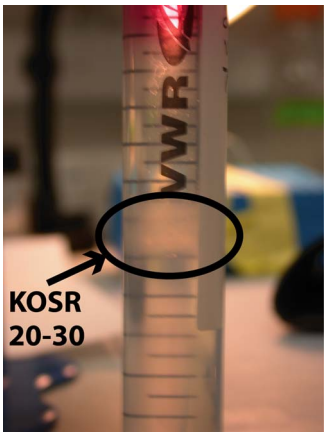

Fig. 3 Density separation of differentiated hESC subpopulations with the Percoll gradient technique. For this figure, chondro-induction was achieved with KOSR. Differentiated hESCs were centrifuged through Percoll solutions ranging from 10% to 60%, and the cell interface between each density layer was counted and seeded for cytocompression testing. The majority of the KOSR cells (52.7%) fell within the 20–30% density interfaces.

Representative creep curves for undifferentiated and differentiated hESCs and native ACs are shown in Fig. 4. Creep cytocompression testing of cell subpopulations from both differentiation regimens resulted in a spectrum of mechanical properties ranging from undifferentiated hESCs to MSCs to ACs (Fig. 5).

The instantaneous moduli values were 0.53 ± 0.33 kPa, 1.03 ± 0.33 kPa, 1.71 ± 0.63 kPa, 1.83 ± 0.75 kPa, 0.85 ± 0.25 kPa, 0.52 ± 0.11 kPa, 1.16 ± 0.53 kPa, and 1.33 ± 0.37 kPa for hESC, TGF 20-30, TGF 30-40, TGF 40-50, KOSR 20-30, KOSR 30-40, MSC, and AC groups, respectively. Differences in E_o were observed between differentiation regimens, among the TGF-β1 subpopulations, and between hESC and all TGF-β1 groups. Moreover, both the TGF 30-40 and 40-50 groups were not different in E_o from the AC group.

The relaxed moduli values were 0.37 ± 0.20 kPa, 0.71 ± 0.26 kPa, 1.04 ± 0.40 kPa, 1.09 ± 0.44 kPa, 0.63 ± 0.20 kPa, 0.44 ± 0.07 kPa, 0.73 ± 0.43 kPa, and 1.14 ± 0.31 kPa for hESC, TGF 20-30, TGF 30-40, TGF 40-50, KOSR 20-30, KOSR 30-40, MSC, and AC groups, respectively. Differences in E_∞ were observed between differentiation regimens, among the TGF-β1 subpopulations, and between hESC and all TGF-β1 groups, and the KOSR 20-30 group. In addition, the TGF 30-40 and 40-50 groups were not different in E_∞ from MSC and AC groups. Notably, the E_∞ of ACs was also greater than MSCs.

The apparent viscosity values were 0.43 ± 0.44 kPa s, 0.53 ± 0.38 kPa s, 1.66 ± 1.63 kPa s, 1.58 ± 1.48 kPa s, 0.54 ± 0.49 kPa s, 0.58 ± 0.48 kPa s, 1.20 ± 0.93 kPa s, and 0.99 ± 1.05 kPa s for hESC, TGF 20-30, TGF 30-40, TGF 40-50, KOSR 20-30, KOSR 30-40, MSC, and AC groups, respectively. Differences in apparent viscosity were observed between hESC and TGF 30-40 and TGF 40-50 groups. In addition, the TGF 30-40 and TGF 40-50 groups were not different from the MSC and AC groups.

The creep time constant values were 2.32 ± 1.92 s, 2.50 ± 1.47 s, 6.03 ± 2.44 s, 5.97 ± 2.17 s, 2.75 ± 1.82 s, 3.84 ± 1.96 s, 5.13 ± 3.79 s, and 3.69 ± 2.95 s for hESC, TGF 20-30, TGF 30-40, TGF 40-50, KOSR 20-30, KOSR 30-40, MSC, and AC groups, respectively. The time constant values of the TGF 30-40, TGF 40-50, and MSC groups were found to be greater than the hESC group, suggestive of a longer time to reach equilibrium deformation under compression. In addition, only the TGF 30-40 group was different from the AC group.

The morphological characteristics of the hESCs, as described by the ratio of cell height to width, changed as a result of the differentiation process and fell within the range of MSCs to ACs (Fig. 6). The cell height: width values were 0.34 ± 0.14, 0.63 ± 0.25, 0.63 ± 0.18, 0.72 ± 0.31, 0.63 ± 0.17, 0.65 ± 0.18, 0.44 ± 0.11, 0.82 ± 0.18 for hESC, TGF 20-30, TGF 30-40, TGF 40-50, KOSR 20-30, KOSR 30-40, MSC, and AC groups, respectively. Moreover, the TGF 40-50 and KOSR 30-40 groups were not different from ACs. For comparison, cell height values were 7.30 ± 2.59, 8.89 ± 3.31, 8.12 ± 1.30, 8.73 ± 3.56, 8.23 ± 3.51, 10.3 ± 2.56, 6.92 ± 1.34, 9.41 ± 2.07 for hESC, TGF 20-30, TGF 30-40, TGF 40-50, KOSR 20-30, KOSR 30-40, MSC, and AC groups, respectively.

Table 1 Distribution of cells isolated at each Percoll gradient interface for cells differentiated using either TGF-β1 or KOSR. Values are given as a percentage of the total cells collected from the entire gradient.

Percoll interface	TGF	KOSR
Top (0–10%)	0.57	0.38
10–20%	2.82	6.54
20–30%	22.60	52.69
30–40%	50.28	27.31
40–50%	16.95	9.23
50–60%	4.52	3.08
Bottom (60%)	2.26	0.77

4 Discussion

The use of hESCs in regenerative medicine is an exciting approach with direct applications to tissue engineering. This study was designed to examine the mechanical properties of hESCs and chondrogenically differentiated hESC subpopulations, using MSCs and ACs as controls. Two differentiation regimens (TGF-β1 or KOSR) were utilized, and the resulting subpopulations were separated based on cell density. Confirming our hypotheses, this study presents several notable findings relating to cellular mechanics and chondrogenic differentiation. First, the mechanical characteristics of single hESCs were investigated and directly compared with native human MSCs and ACs. Second, the density gradient technique was successfully employed to separate cell subpopulations with distinct mechanical properties. Finally, a subpopulation of differentiated hESCs was identified with similar mechanical and morphological properties as native chondrocytes.

To our knowledge, this is the first study to examine the mechanical properties of single hESCs, a necessary step toward understanding the role of mechanical factors in cellular homeostasis and differentiation. It is well established that hESCs are mechanosensitive cells and respond differentially to applied forces or their three-dimensional mechanical environment [10,12]. For instance, previous research has employed dynamic compression [13] and hydrostatic pressure [34] as successful differentiation agents for hESC chondrogenesis. In addition, changes in substrate rigidity and scaffold porosity, which are intimately linked with the transduction of forces on to single cells, can promote a desired embryonic stem cell differentiation [35]. Therefore, an understanding of the mechanical properties of hESCs may greatly aid research toward identifying an appropriate loading regimen and mechanical environment, which induce a favorable cellular differentiation. In the future, this information can be coupled with traditional biochemical differentiation agents, such as growth factors, to optimize hESC differentiation approaches in the laboratory.

The reported hESC characteristics were directly compared with MSCs and native ACs to yield the "mechanical range" of single cells along the chondrogenic lineage. Phenotypic changes during chondrogenesis are manifested by changes in cytoskeletal structure and cellular morphology [36–39], which in turn contribute substantially to altered cellular mechanics [32,40]. Examining me-

Downloaded From: http://biomechanical.asmedigitalcollection.asme.org/ on 06/19/2015 Terms of Use: http://asme.org/terms

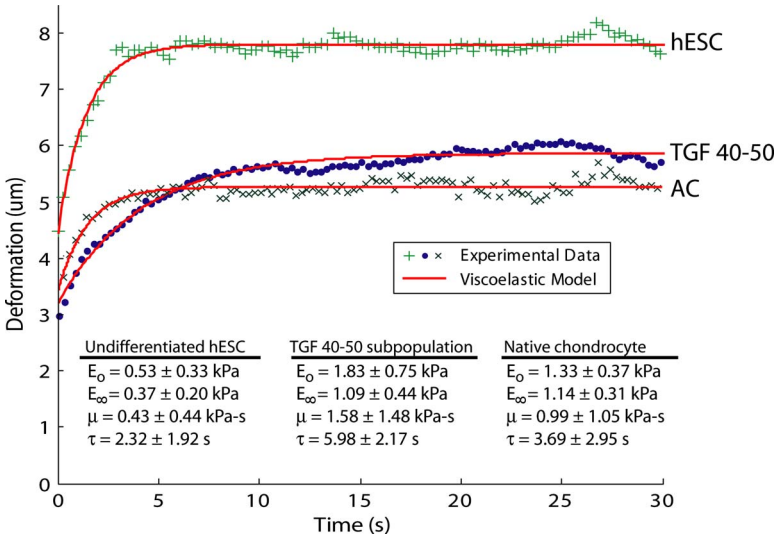

Fig. 4 Representative creep curves of single cells. The experimental data points were fitted to a viscoelastic model to yield an instantaneous modulus, relaxed modulus, apparent viscosity, and a creep time constant. Undifferentiated hESCs typically exhibited a greater deformation, suggestive of a lower stiffness, and a faster time to equilibrium, suggestive of a lower apparent viscosity and time constant than differentiated hESCs (example shown from TGF 40-50 group) in response to the same applied load. In addition, the equilibrium deformation of single cells from the TGF 40-50 subpopulation was akin to that of native chondrocytes, indicative of their similar stiffness values. For clarity, only one out of every 1000 experimental data points is shown for each curve. Representative cells were of 12 μm height.

chanical changes during cartilage development on the single cell level sheds light on the role of biomechanical factors in healthy tissue formation and maintenance of the cellular microenvironment [11]. In this experiment, cells became more rounded with differentiation to suggest continued rearrangement of the cytoskeleton. Moreover, parallels between the progression of cellular phenotype and mechanics can be drawn. It was found that the instantaneous modulus of hESCs was approximately 45% and 40% that of MSCs and ACs, respectively. In terms of the relaxed modulus, increases were observed from hESCs to MSCs (~2-fold) and from MSCs to ACs (~1.5-fold). Thus, cellular stiffening appears to coincide with chondrodifferentiation. Moreover, the observed differences in stiffness properties between hESCs, MSCs, and ACs may be indicative of the types of forces each of the cells typically is exposed to in vivo. For instance, mature native ACs must withstand high compressive loading in articular cartilage [41] and therefore need to be stiffer, while hESCs or MSCs experience primarily nondeformational hydrostatic forces, although at different levels, in the developing embryo or limb bud [11].

Density separation was successfully utilized to isolate cell subpopulations with different mechanical properties. It is of great interest to identify an effective methodology to purify nonhomogeneous cell populations for use in tissue engineering. Both differentiation methods yielded subpopulations with properties distributed along the mechanical range from hESCs to ACs. For example, the instantaneous modulus of TGF 20-30 cells was akin to that of MSCs, while the TGF 40-50 subpopulation was similar only to ACs. Interestingly, no differences in cell morphology (e.g., cell height and diameter) were observed among the separated hESC subpopulations, suggesting that the mechanical differences were related to cytoskeletal and organelle densities. In light of this counterintuitive finding, mechanics may be a finer tool to detect differences among cell populations. Thus, it is particularly exciting to observe, for the first time, that the density separation can be utilized to isolate cells with unique mechanical properties. Therefore, future studies should compare this separation technique to more traditional cell sorting methodologies, such as fluorescence-activated cell sorting (FACS) and magnetic-activated cell separation (MACS) [42,43].

Unconfined cytocompression was then employed to identify a subpopulation of differentiated hESCs potentially suitable for articular cartilage tissue engineering. While all of the differentiated hESC subpopulations were more rounded than undifferentiated hESCs, only the TGF 40-50 and KOSR 30-40 groups were not morphologically different from ACs. Of these two groups, only the TGF 40-50 subpopulation was similar to ACs with regards to all viscoelastic material parameters. Moreover, TGF 40-50 cells were fourfold higher in apparent viscosity than undifferentiated hESCs, which is suggestive of a transformation from elastic to viscoelastic mechanical behavior [8]. This coincides with previous research demonstrating the important role of vimentin intermediate filaments, minimally present in hESCs, in maintaining the chondrocyte phenotype [36] and a viscoelastic response to an applied load [40]. Identification of a differentiated hESC subpopulation with similar mechanical properties as native chondrocytes may provide utility in tissue engineering. These cells will need to withstand any mechanical stimulation regimen employed to augment the functional characteristics of engineered tissue [44], as well as the highly mechanical environment in the native joint [41]. If the cells are too soft, they may experience nonphysiologically high strain levels during normal loading activity. It has been shown that mechanical behavior of chondrocytes is strain-dependent and that beyond a critical point cells can no longer recover from the applied strain, suggestive of a breakdown in the cytoskeleton or other pathogenic changes [19]. Conversely, if the differentiated hESCs are too stiff, the necessary levels of mechanical stimulation may not be reached to maintain chondrocyte homeostasis [45]. Thus, the TGF 40-50 subpopulation may prove to be a valuable cell source for cartilage regeneration.

Creep cytocompression is a powerful methodology to infer changes in cell physiology, as long as the results are taken within

Downloaded From: http://biomechanical.asmedigitalcollection.asme.org/ on 06/19/2015 Terms of Use: http://asme.org/terms

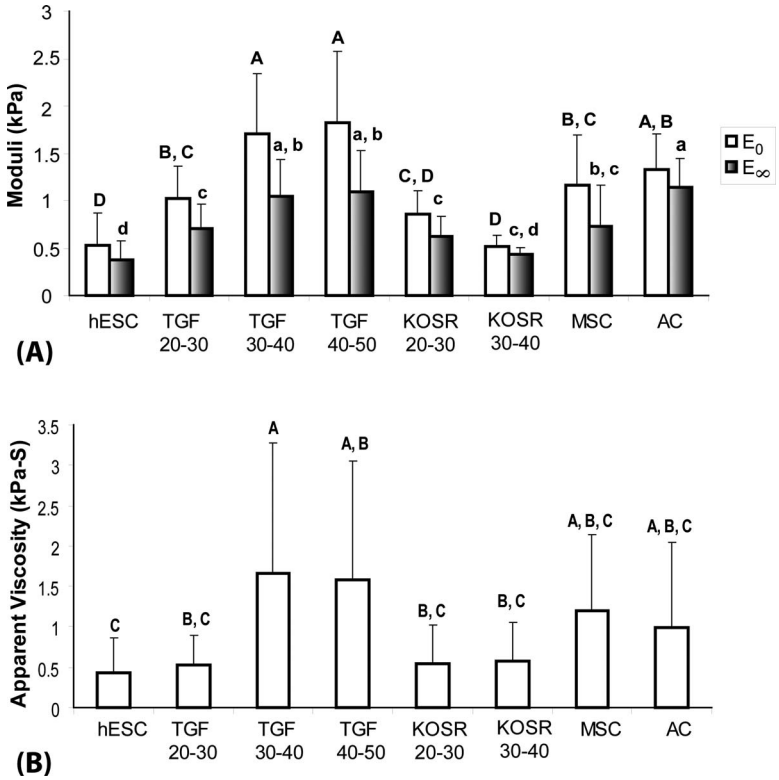

Fig. 5 Viscoelastic material properties of undifferentiated and differentiated single hESCs, as well as mesenchymal stem cell and articular chondrocyte controls. Differences in instantaneous and relaxed moduli were observed between density interfaces (TGF 20-30 versus TGF 30-40, or TGF 40-50), differentiation regimens (TGF-β1 versus KOSR), and differentiation state (hESC versus MSC versus TGF 40-50) (*a*). Moreover, differentiated cell subpopulations (TGF 30-40 and TGF 40-50) were identified which were not different than native ACs. In addition, the apparent viscosities of the TGF 30-40 and TGF 40-50 groups were greater than that of undifferentiated hESCs (*b*). Data presented as mean ± standard deviations.

the appropriate context. The behavior of individual cells seeded on a Petri dish can potentially be quite different to that of cells distributed within extracellular matrix. For instance, the microenvironment of chondrocytes has been shown to significantly influence the transmission of forces around individual cells [46]. Moreover, testing single cells does not consider the role of cell communication and the transmission of signaling molecules in the response of cells to an applied force [47]. An additional limitation

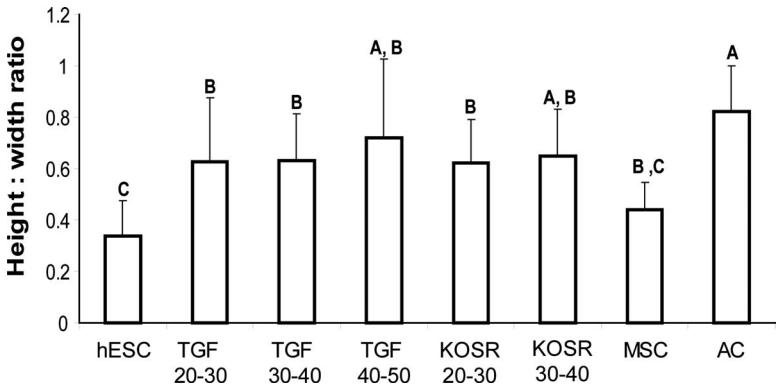

Fig. 6 Morphological properties of undifferentiated and differentiated single hESCs, as well as mesenchymal stem cell and articular chondrocyte controls. The cell height-to-width ratios of all differentiated cell subpopulations were greater than that of undifferentiated hESCs and approaching 1.0, which is indicative of a more rounded cell morphology. The values for differentiated hESCs all fell between the range of MSCs and ACs. Moreover, there was no difference between the cell height-to-width ratio of the TGF 40-50 and KOSR 30-40 cells and native ACs. Data presented as mean ± standard deviations.

Downloaded From: http://biomechanical.asmedigitalcollection.asme.org/ on 06/19/2015 Terms of Use: http://asme.org/terms

is in regards to the assumptions necessary to yield viscoelastic properties to describe the cell. In this study, cells were considered to be homogeneous, isotropic, and incompressible materials. While all cell types are unquestionably complex arrangements of organelles, cytoskeletal structures, and nuclear components, the previous assumptions in material behavior facilitate ease in data analysis and allow for consistent comparisons across all experimental groups. Despite the aforementioned caveats, approaches in single cell mechanics have been successfully utilized to distinguish cells based on zonal arrangement within a tissue [5,31], pathogenic state [48], and phenotype [4]. Thus, mechanical differences between single cell populations may be retained after isolation in vitro and may not be entirely dependent on the cellular microenvironment and biochemical factors. Moreover, the creep curves generated for all groups in this study fit well to the theoretical viscoelastic model employed. Taking these considerations in tandem, single cell mechanical testing may be a suitable method to identify changes indicative of hESC chondrogenesis.

This study identifies cellular mechanics as an important marker for phenotypic changes. We have elucidated mechanical and morphological differences between hESCs, MSCs, and ACs, which may be indicative of changes in intracellular structures or the cellular mechanical environment during chondrogenesis. Using a density separation technique, we were able to distinctly isolate subpopulations with unique mechanical characteristics. Furthermore, from these subpopulations, we identified one group of differentiated hESCs with similar mechanical properties as native ACs, which may be useful in future cartilage tissue engineering efforts. An understanding of the mechanical characteristics of undifferentiated and differentiated hESCs may have implications toward elucidating the role of physical forces in promoting specific cellular phenotypes.

Acknowledgment

G.O. and V.P.W. contributed equally in this work. We would like to gratefully acknowledge funding from NIAMS (Grant No. R01 AR053286), NIH (training fellowship for Mr. Ofek, Grant Nos. 5 T90 DK70121-03 and 5 R90 DK71504-03), and NSF (training fellowship for Dr. Koay, Grant No. DGE-0114264). We also thank Dr. Christopher P. Cannon's invaluable assistance in procuring the human articular cartilage. Some of the materials employed in this work were provided by the Tulane Center for Gene Therapy through a grant from NCRR of the NIH, Grant No. P40RR017447.

References

[1] Guilak, F., and Mow, V. C., 2000, "The Mechanical Environment of the Chondrocyte: A Biphasic Finite Element Model of Cell-Matrix Interactions in Articular Cartilage," J. Biomech., **33**(12), pp. 1663–1673.
[2] Wang, N., Butler, J. P., and Ingber, D. E., 1993, "Mechanotransduction Across the Cell Surface and Through the Cytoskeleton," Science, **260**(5111), pp. 1124–1127.
[3] Titushkin, I., and Cho, M., 2007, "Modulation of Cellular Mechanics During Osteogenic Differentiation of Human Mesenchymal Stem Cells," Biophys. J., **93**(10), pp. 3693–3702.
[4] Darling, E. M., Topel, M., Zauscher, S., Vail, T. P., and Guilak, F., 2008, "Viscoelastic Properties of Human Mesenchymally-Derived Stem Cells and Primary Osteoblasts, Chondrocytes, and Adipocytes," J. Biomech., **41**(2), pp. 454–464.
[5] Darling, E. M., Zauscher, S., and Guilak, F., 2006, "Viscoelastic Properties of Zonal Articular Chondrocytes Measured by Atomic Force Microscopy," Osteoarthritis Cartilage, **14**(6), pp. 571–579.
[6] Sato, M., Theret, D. P., Wheeler, L. T., Ohshima, N., and Nerem, R. M., 1990, "Application of the Micropipette Technique to the Measurement of Cultured Porcine Aortic Endothelial Cell Viscoelastic Properties," ASME J. Biomech. Eng., **112**(3), pp. 263–268.
[7] Koay, E. J., Shieh, A. C., and Athanasiou, K. A., 2003, "Creep Indentation of Single Cells," ASME J. Biomech. Eng., **125**(3), pp. 334–341.
[8] Leipzig, N. D., and Athanasiou, K. A., 2005, "Unconfined Creep Compression of Chondrocytes," J. Biomech., **38**(1), pp. 77–85.
[9] Darling, E. M., and Athanasiou, K. A., 2005, "Rapid Phenotypic Changes in Passaged Articular Chondrocyte Subpopulations," J. Orthop. Res., **23**(2), pp. 425–32.
[10] Mcbeath, R., Pirone, D. M., Nelson, C. M., Bhadriraju, K., and Chen, C. S., 2004, "Cell Shape, Cytoskeletal Tension, and Rhoa Regulate Stem Cell Lineage Commitment," Dev. Cell, **6**(4), pp. 483–95.
[11] Carter, D. R., Beaupre, G. S., Wong, M., Smith, R. L., Andriacchi, T. P., and Schurman, D. J., 2004, "The Mechanobiology of Articular Cartilage Development and Degeneration," Clin. Orthop. Relat. Res., **427**, pp. S69–S77.
[12] Schumann, D., Kujat, R., Nerlich, M., and Angele, P., 2006, "Mechanobiological Conditioning of Stem Cells for Cartilage Tissue Engineering," Biomed. Mater. Eng., **16**(4), pp. S37–S52.
[13] Terraciano, V., Hwang, N., Moroni, L., Park, H. B., Zhang, Z., Mizrahi, J., Seliktar, D., and Elisseeff, J., 2007, "Differential Response of Adult and Embryonic Mesenchymal Progenitor Cells to Mechanical Compression in Hydrogels," Stem Cells, **25**(11), pp. 2730–2738.
[14] Wu, C. C., Chao, Y. C., Chen, C. N., Chien, S., Chen, Y. C., Chien, C. C., Chiu, J. J., and Linju Yen, B., 2008, "Synergism of Biochemical and Mechanical Stimuli in the Differentiation of Human Placenta-Derived Multipotent Cells Into Endothelial Cells," J. Biomech., **41**(4), pp. 813–821.
[15] Koay, E. J., Hoben, G. M., and Athanasiou, K. A., 2007, "Tissue Engineering With Chondrogenically Differentiated Human Embryonic Stem Cells," Stem Cells, **25**(9), pp. 2183–2190.
[16] Hoben, G. M., Koay, E. J., and Athanasiou, K. A., 2008, "Fibrochondrogenesis in Two Embryonic Stem Cell Lines: Effects of Differentiation Timelines," Stem Cells, **26**(2), pp. 422–430.
[17] Shieh, A. C., and Athanasiou, K. A., 2007, "Dynamic Compression of Single Cells," Osteoarthritis Cartilage, **15**(3), pp. 328–334.
[18] Leipzig, N. D., and Athanasiou, K. A., 2008, "Static Compression of Single Chondrocytes Catabolically Modifies Single-Cell Gene Expression," Biophys. J., **94**(6), pp. 2412–2422.
[19] Koay, E. J., Ofek, G., and Athanasiou, K. A., 2008, "Effects of TGF-β1 and IGF-I on the Compressibility, Biomechanics, and Strain-Dependent Recovery Behavior of Single Chondrocytes," J. Biomech., **41**(5), pp. 1044–52.
[20] Levenberg, S., Huang, N. F., Lavik, E., Rogers, A. B., Itskovitz-Eldor, J., and Langer, R., 2003, "Differentiation of Human Embryonic Stem Cells on Three-Dimensional Polymer Scaffolds," Proc. Natl. Acad. Sci. U.S.A., **100**(22), pp. 12741–12746.
[21] Toh, W. S., Yang, Z., Liu, H., Heng, B. C., Lee, E. H., and Cao, T., 2007, "Effects of Culture Conditions and Bone Morphogenetic Protein 2 on Extent of Chondrogenesis From Human Embryonic Stem Cells," Stem Cells, **25**(4), pp. 950–960.
[22] Hwang, N. S., Varghese, S., Zhang, Z., and Elisseeff, J., 2006, "Chondrogenic Differentiation of Human Embryonic Stem Cell-Derived Cells in Arginine-Glycine-Aspartate-Modified Hydrogels," Tissue Eng., **12**(9), pp. 2695–2706.
[23] Hwang, N. S., Kim, M. S., Sampattavanich, S., Baek, J. H., Zhang, Z., and Elisseeff, J., 2006, "Effects of Three-Dimensional Culture and Growth Factors on the Chondrogenic Differentiation of Murine Embryonic Stem Cells," Stem Cells, **24**(2), pp. 284–91.
[24] Koay, E. J., and Athanasiou, K. A., "Development of Serum-Free, Chemically Defined Conditions for Human Embryonic Stem Cell-Derived Fibrochondrogenesis," Tissue Eng. Part A (to be published).
[25] Itskovitz-Eldor, J., Schuldiner, M., Karsenti, D., Eden, A., Yanuka, O., Amit, M., Soreq, H., and Benvenisty, N., 2000, "Differentiation of Human Embryonic Stem Cells Into Embryoid Bodies Compromising the Three Embryonic Germ Layers," Mol. Med., **6**(2), pp. 88–95.
[26] Pawlowski, A., Makower, A. M., Madsen, K., Wroblewski, J., and Friberg, U., 1986, "Cell Fractions From Rat Rib Growth Cartilage. Biochemical Characterization of Matrix Molecules," Exp. Cell Res., **164**(1), pp. 211–22.
[27] Min, B. H., Kim, H. J., Lim, H., and Park, S. R., 2002, "Characterization of Subpopulated Articular Chondrocytes Separated by Percoll Density Gradient," In Vitro Cell. Dev. Biol.: Anim., **38**(1), pp. 35–40.
[28] Wong, M., and Tuan, R. S., 1995, "Interactive Cellular Modulation of Chondrogenic Differentiation In Vitro by Subpopulations of Chick Embryonic Calvarial Cells," Dev. Biol., **167**(1), pp. 130–147.
[29] Zhang, S. C., Wernig, M., Duncan, I. D., Brustle, O., and Thomson, J. A., 2001, "In Vitro Differentiation of Transplantable Neural Precursors From Human Embryonic Stem Cells," Nat. Biotechnol., **19**(12), pp. 1129–1133.
[30] Patella, V., Marino, I., Lamparter, B., Arbustini, E., Adt, M., and Marone, G., 1995, "Human Heart Mast Cells. Isolation, Purification, Ultrastructure, and Immunologic Characterization," J. Immunol., **154**(6), pp. 2855–2865.
[31] Shieh, A. C., and Athanasiou, K. A., 2006, "Biomechanics of Single Zonal Chondrocytes," J. Biomech., **39**(9), pp. 1595–1602.
[32] Leipzig, N. D., Eleswarapu, S. V., and Athanasiou, K. A., 2006, "The Effects of TGF-β1 and IGF-I on the Biomechanics and Cytoskeleton of Single Chondrocytes," Osteoarthritis Cartilage, **14**(12), pp. 1227–1236.
[33] Rosenberg, L., 1971, "Chemical Basis for the Histological Use of Safranin O in the Study of Articular Cartilage," J. Bone Jt. Surg., Am. Vol., **53**(1), pp. 69–82.
[34] Angele, P., Yoo, J. U., Smith, C., Mansour, J., Jepsen, K. J., Nerlich, M., and Johnstone, B., 2003, "Cyclic Hydrostatic Pressure Enhances the Chondrogenic Phenotype of Human Mesenchymal Progenitor Cells Differentiated In Vitro," J. Orthop. Res., **21**(3), pp. 451–457.
[35] Taqvi, S., and Roy, K., 2006, "Influence of Scaffold Physical Properties and Stromal Cell Coculture on Hematopoietic Differentiation of Mouse Embryonic Stem Cells," Biomaterials, **27**(36), pp. 6024–6031.
[36] Blain, E. J., Gilbert, S. J., Hayes, A. J., and Duance, V. C., 2006, "Disassembly of the Vimentin Cytoskeleton Disrupts Articular Cartilage Chondrocyte Homeostasis," Matrix Biol., **25**(7), pp. 398–408.
[37] Brown, P. D., and Benya, P. D., 1988, "Alterations in Chondrocyte Cytoskeletal Architecture During Phenotypic Modulation by Retinoic Acid and Dihy-

Downloaded From: http://biomechanical.asmedigitalcollection.asme.org/ on 06/19/2015 Terms of Use: http://asme.org/terms

drocytochalasin B-Induced Reexpression," J. Cell Biol., **106**(1), pp. 171–179.
[38] Loty, S., Forest, N., Boulekbache, H., and Sautier, J. M., 1995, "Cytochalasin D Induces Changes in Cell Shape and Promotes In Vitro Chondrogenesis: A Morphological Study," Biol. Cell, **83**(2–3), pp. 149–161.
[39] Vinall, R. L., Lo, S. H., and Reddi, A. H., 2002, "Regulation of Articular Chondrocyte Phenotype by Bone Morphogenetic Protein 7, Interleukin 1, and Cellular Context is Dependent on the Cytoskeleton," Exp. Cell Res., **272**(1), pp. 32–44.
[40] Trickey, W. R., Vail, T. P., and Guilak, F., 2004, "The Role of the Cytoskeleton in the Viscoelastic Properties of Human Articular Chondrocytes," J. Orthop. Res., **22**(1), pp. 131–139.
[41] Mow, V. C., and Ratcliffe, A., 1997, "Structure and Function of Articular Cartilage and Meniscus," *Basic Orthopaedic Biomechanics*, Lippincott-Raven, Philadelphia, PA.
[42] Adams, J. D., Kim, U., and Soh, H. T., 2008, "Multitarget Magnetic Activated Cell Sorter," Proc. Natl. Acad. Sci. U.S.A., **105**(47), pp. 18165–18170.
[43] Fickert, S., Fiedler, J., and Brenner, R. E., 2004, "Identification of Subpopulations With Characteristics of Mesenchymal Progenitor Cells From Human Osteoarthritic Cartilage Using Triple Staining for Cell Surface Markers," Arthritis Res. Ther., **6**(5), pp. R422–R432.
[44] Aufderheide, A. C., and Athanasiou, K. A., 2004, "Mechanical Stimulation Toward Tissue Engineering of the Knee Meniscus," Ann. Biomed. Eng., **32**(8), pp. 1163–1176.
[45] Freeman, P. M., Natarajan, R. N., Kimura, J. H., and Andriacchi, T. P., 1994, "Chondrocyte Cells Respond Mechanically to Compressive Loads," J. Orthop. Res., **12**(3), pp. 311–320.
[46] Alexopoulos, L. G., Setton, L. A., and Guilak, F., 2005, "The Biomechanical Role of the Chondrocyte Pericellular Matrix in Articular Cartilage," Acta Biomater., **1**(3), pp. 317–325.
[47] D'andrea, P., Calabrese, A., Capozzi, I., Grandolfo, M., Tonon, R., and Vittur, F., 2000, "Intercellular Ca2+Waves in Mechanically Stimulated Articular Chondrocytes," Biorheology, **37**(1–2), pp. 75–83.
[48] Trickey, W. R., Lee, G. M., and Guilak, F., 2000, "Viscoelastic Properties of Chondrocytes From Normal and Osteoarthritic Human Cartilage," J. Orthop. Res., **18**(6), pp. 891–898.

Downloaded From: http://biomechanical.asmedigitalcollection.asme.org/ on 06/19/2015 Terms of Use: http://asme.org/terms